

## Specificity and Inhibitory Mechanism of Andrographolide and Its Analogues as Antiasthma Agents on NF- $\kappa$ B p50

Van Sang Nguyen,<sup>†,‡</sup> Xin Yi Loh,<sup>‡</sup> Hadhi Wijaya,<sup>§</sup> Jigang Wang,<sup>†</sup> Qingsong Lin,<sup>†</sup> Yulin Lam,<sup>§</sup> Wai-Shiu Fred Wong,<sup>‡</sup> and Yu Keung Mok<sup>\*,†</sup>

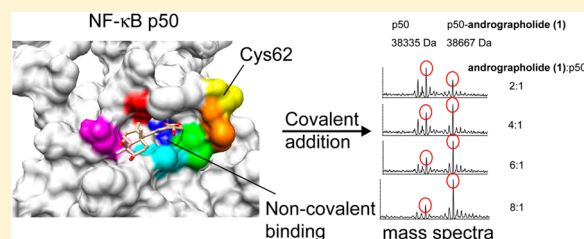
<sup>†</sup>Department of Biological Sciences, National University of Singapore, 14 Science Drive 4, Singapore 117543

<sup>‡</sup>Department of Pharmacology, Yong Loo Lin School of Medicine, National University Health System, Singapore and Immunology Program, Life Science Institute, National University of Singapore, Singapore 117456

<sup>§</sup>Department of Chemistry, National University of Singapore, Singapore 117543

### S Supporting Information

**ABSTRACT:** Andrographolide (**1**) is a diterpenoid lactone with an  $\alpha,\beta$ -unsaturated lactone group that inhibits NF- $\kappa$ B DNA binding. Andrographolide reacts with the nucleophilic Cys62 of NF- $\kappa$ B p50 through a Michael addition at the  $\Delta^{12(13)}$  exocyclic double bond to form a covalent adduct. Using computer docking, site-directed mutagenesis, and mass spectrometry, the noncovalent interactions between andrographolide and additional binding site residues other than Cys62 were found to be essential for the covalent incorporation of andrographolide. Furthermore, the addition reaction of andrographolide on Cys62 was highly dependent on the redox conditions and on the vicinity of nearby, positively charged Arg residues in the conserved RxxRxxR motif. The reaction mechanisms of several of the analogues were determined, showing that 14-deoxy-11,12-didehydroandrographolide (**8**) reacts with NF- $\kappa$ B p50 via a novel mechanism distinct from andrographolide. The noncovalent interaction and redox environment of the binding site should be considered, in addition to the electrophilicity, when designing a covalent drug. Analogues similar in structure appear to use distinct reaction mechanisms and may have very different cytotoxicities, e.g., compound **6**.



NF- $\kappa$ B is a pro-survival transcription factor maintained in its inactive form in complex with the I $\kappa$ B inhibitor. NF- $\kappa$ B consists of homo- and heterodimers of the p50 and p65 subunits. The p50 subunit (50 kDa) contains a 300-residue region in its N-terminus that is highly homologous with the Rel homology region (RHR), an oncogene from the reticuloendotheliosis virus of turkeys. The RHR comprises an N-terminal (Rel-N) portion and a C-terminal dimerization domain (Rel-C) joined by a short, flexible 10-residue linker. The NF- $\kappa$ B p65 subunit (65 kDa, also known as Rel-A) also contains an RHR and an additional transcriptional activation domain at its extreme C-terminus, which is not found in p50.<sup>1</sup> The Rel-N and the Rel-C domains follow the immunoglobulin fold, with 10 flexible loops that extend from the secondary structure of these domains to contact DNA.

The crystal structures of the p50–p65 heterodimer,<sup>2,3</sup> the p65–p65 homodimer,<sup>4</sup> and the p50–p50 homodimer<sup>5,6</sup> have been determined previously. The p50–p65 heterodimer is the predominant form and binds to the  $\kappa$ B DNA with a  $K_d$  of  $\sim$ 10 nM; p50 and p65 homodimers bind with 5- and 15-fold lower affinities, respectively.<sup>7</sup> NF- $\kappa$ B binds to a 10-base-pair consensus sequence, 5'-GGGRNYYYCC-3',<sup>8</sup> at the promoter regions of various genes involved in numerous pathologies,<sup>9</sup> with NF- $\kappa$ B hyperactivation identified in inflammatory diseases, neurodegenerative disorders, and cancers in humans.<sup>10</sup> Thus, small-molecule inhibitors of NF- $\kappa$ B or proteins that act along

its signaling and regulatory pathways may provide an important therapeutic strategy.<sup>10</sup>

Andrographolide (**1**) and its analogues are labdane diterpenoids isolated from *Andrographis paniculata* Nees (Acanthaceae) that are used as herbal drugs in the People's Republic of China and India against inflammatory diseases and cancer.<sup>11</sup> Andrographolide (**1**) is an electrophilic,  $\alpha,\beta$ -unsaturated  $\gamma$ -lactone capable of forming covalent bonds with nucleophilic centers in proteins, such as those with cysteine residues.<sup>12</sup> Indeed, **1** belongs to the Michael acceptor system category of electrophilic natural products<sup>13</sup> and covalently attaches to the conserved Cys62 residue at the N-terminus of NF- $\kappa$ B p50.<sup>14</sup> This Cys62 is more susceptible to redox changes than the other Cys residues, likely due to the presence of the adjacent "RxxRxxR" motif.<sup>15</sup> Using free and reduced glutathione (GSH), studies have shown that the  $\alpha,\beta$ -unsaturated lactone moiety of **1** reacts with GSH through a Michael addition at the  $\Delta^{12(13)}$  exocyclic double bond followed by dehydration of the adduct.<sup>16,17</sup>

Previous work identified a novel anti-inflammatory role for andrographolide (**1**) in asthma via inhibition of the NF- $\kappa$ B pathway.<sup>18</sup> Later, a noncytotoxic natural analogue of **1**, 14-

Received: September 25, 2014

deoxy-11,12-didehydroandrographolide (**8**), was identified and shown to retain the anti-inflammatory effects against asthma, likely through NF- $\kappa$ B inhibition.<sup>19</sup> The analogue 4-hydroandrographolide (4H-andro), which lacks the  $\Delta^{12(13)}$  exocyclic double bond, is inactive in attenuating inflammation<sup>14</sup> or suppressing the proliferation of arterial neointima.<sup>20</sup> In addition to natural analogues of **1**, various synthesized analogues have been produced by modifying the  $\alpha,\beta$ -unsaturated  $\gamma$ -butyrolactone moiety, the two double bonds  $\Delta^{8(17)}$  and  $\Delta^{12(13)}$ , and the three hydroxy groups at C-3 (secondary), C-14 (allylic), and C-19 (primary). Some of these analogues have improved cytotoxic activity toward cancer cell lines, such as the 19-*O*-triphenylmethyl ether analogue;<sup>21</sup> the dispiropyrrrolizidino oxindole derivative;<sup>22</sup> and the SRS07 derivative<sup>23</sup> of **1**. However, the mechanisms of reaction and determinants of reactivity of these analogues with p50 are unknown.

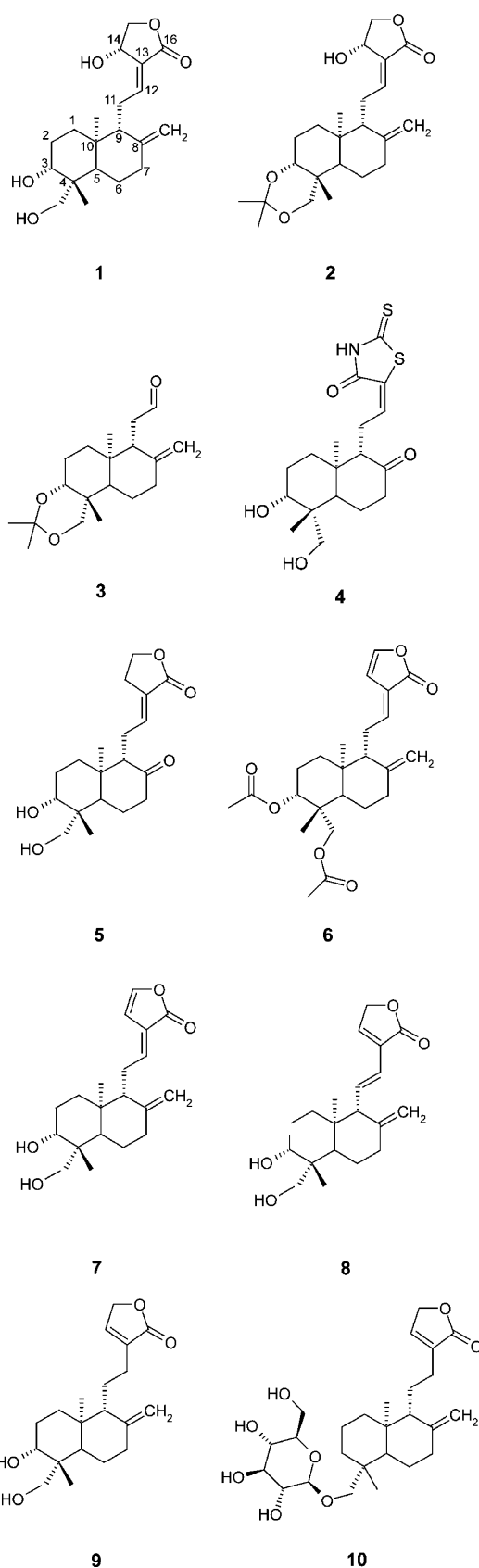
On the basis of computational docking simulations and site-directed mutagenesis, here we report the first direct evidence for a specific binding site of andrographolide (**1**) on the NF- $\kappa$ B p50 subunit next to Cys62. This binding site, in addition to the nucleophilicity of Cys62, is essential for **1** to target Cys62 rather than other Cys residues in the subunit. Mass spectrometry and cell analyses determined the relative reactivity of different analogues of **1** to p50 *in vitro*. The unexpected shift in the molecular weights of adducts formed by analogues of **1** with NF- $\kappa$ B p50 provides insights into their mechanisms of interaction. Binding of **1** to NF- $\kappa$ B p50 is highly dependent on the redox state of Cys62, and the covalent adduct can be dissociated in the presence of dithiothreitol (DTT). The data in this study improve our understanding of how this class of compound interacts with targets and will aid in the design of analogues of **1** and other electrophilic natural products for the treatment of various human pathologies.

## RESULTS AND DISCUSSION

### The Noncovalent Binding Site of Andrographolide (**1**) on NF- $\kappa$ B p50 Is Essential for Its Covalent Interaction.

Mass spectrometric analyses have previously shown the covalent attachment of electrophilic **1** to the conserved nucleophilic Cys62 residue at the N-terminal domain (NTD) of the NF- $\kappa$ B p50 subunit through Michael addition.<sup>14</sup> However, the reaction of **1** with Cys62 of p50 may be not only dependent on the intrinsic electrophilicity of **1** but also partially dependent on matching the shape and property of the drug with a specific binding site next to Cys62. To predict the possible binding site of **1** on p50, a docking experiment was carried out using iGEMDOCK 2.1.<sup>24</sup> One hundred runs were performed using the “accurate docking” parameters, and the 100 conformers tended to be located in close vicinity to each other on the p50 NTD (Figure 1A). Among these 100 conformers, 67 of the lowest energy conformers formed a very well-defined single major cluster in a cavity next to Cys62 (Figure 1B), the binding pocket of which mainly comprised four hydrophobic residues (Val61, Val115, Ile142, and Leu143) along with Ser66 and Asn139.

Using mass spectrometry, the extent of the reaction was determined based on the amount of adduct that formed between p50 NTD and increasing concentrations of **1**. Andrographolide (**1**) was found to react with wild-type p50 NTD in a concentration-dependent manner, reaching saturation at a molar ratio of  $\sim$ 8:1 (**1**:p50) (Figure 2A). The molecular weight of the adduct was determined as 38 667 Da, which is 18 Da less than the combined molecular weight of p50



(38 335 Da) and **1** (350 Da), suggesting removal of a water molecule during the reaction. This finding agrees with the previously suggested mechanism of the reaction between GSH and **1**, in which the  $\alpha,\beta$ -unsaturated lactone moiety of **1** reacts with GSH through a Michael addition followed by dehydration

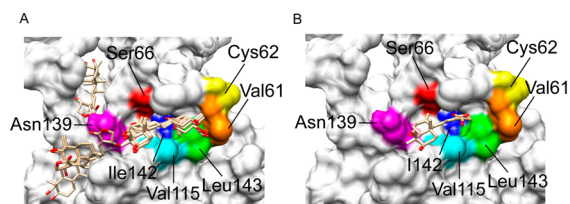


**Figure 1.** Docking of andrographolide (**1**) on NF- $\kappa$ B p50. Blind docking (rigid residues) was performed using iGEMdock v2.1<sup>24</sup> with 100 solutions. (A) The 100 conformers docked around a site adjacent to Cys62. The binding site residues are colored: Val61 (orange); Cys62 (yellow); Ser66 (red); Val115 (cyan); Asn139 (magenta); Ile142 (blue); Leu143 (green). (B) When the 100 conformers were sorted according to their energies, 67 conformers with the lowest energies formed a single cluster. The double bond between C-12 and C-13 of **1** points toward residue Cys62 to allow nucleophilic attack by the SH group. The figures were generated using the program Chimera.<sup>25</sup>

of the adduct.<sup>17</sup> On the basis of the docking model, the binding site for **1** comprises mainly hydrophobic residues (Val115, Ile142, and Leu143) from  $\beta$ H and L2 and polar residues (Ser66 and Asn139) from L1 and  $\beta$ E'.<sup>6</sup> The location and orientation of

**1** allow for the nucleophilic attack of the  $\Delta^{12(13)}$  exocyclic double bond of **1** by the side-chain SH group of Cys62.

To test the importance of the six binding site residues (Val61, Val115, Ile142, Leu143, Ser66, and Asn139) in the binding pocket, six alanine substitution mutants were prepared, as well as a C62A mutant. The reactivity of these seven p50 NTD mutants with **1** was determined using mass spectrometry. As expected, no reaction was observed between **1** and the C62A p50 NTD mutant (Figure 2B). Similarly, the I142A mutant of p50 NTD also showed no reaction with **1** up to a molar ratio of 10:1 (1:p50 NTD) (Figure 2D). Further, a significant reduction in the extent of the reaction (based on adduct formation as compared with the unbound form) for the S66A mutant was observed across the range of concentrations tested (Figure 2C), but none of the other mutants affected the extent of the reaction (Figure 2E). The far-UV CD spectra and thermal stabilities of the S66A and I142A mutants were similar to that of wild-type p50 NTD (see Supporting Information), suggesting that the reduced reaction was not due to protein denaturation but due to the loss of the specific interaction of the side-chain of these binding site residues with **1**.

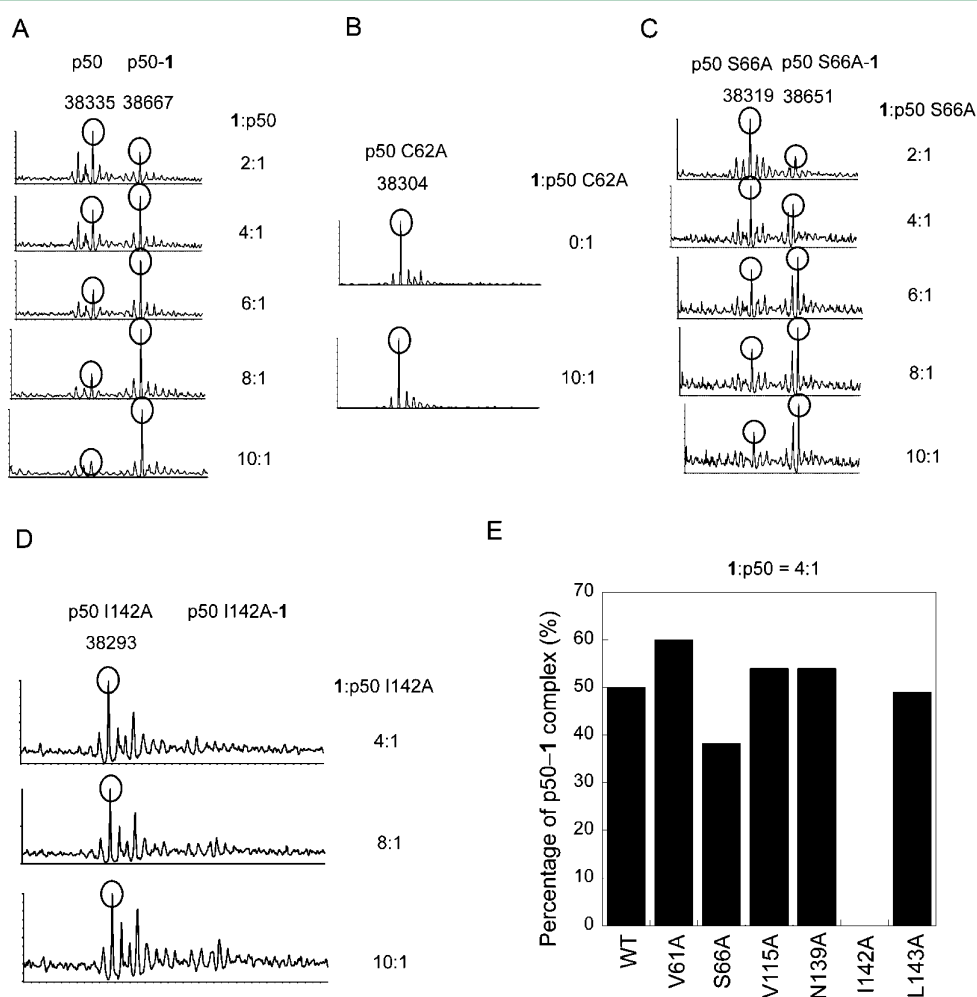


**Figure 2.** Reactivity of andrographolide (**1**) with site-directed mutants of NF- $\kappa$ B p50. Series of mass spectra showing the reaction of **1** with (A) wild-type p50, (B) C62A, (C) S66A, and (D) I142A mutants of p50. The peaks of free p50 and the p50-**1** adducts are marked with black circles with their respective molecular weights shown above. The molar ratios of 1:p50 are shown at the right-hand side of each mass spectrum. (E) Bar chart showing the percentage of p50-**1** complex formed by the wild-type and mutants of p50 at a molar ratio of 4:1 (1:p50). The percentage of complex formed = (peak height of p50-**1** complex / (peak height of free p50 + peak height of p50-**1** complex))  $\times$  100.

A recent review suggests that inhibition of target protein by covalent drugs occurs in two steps.<sup>26</sup> First, the compound binds noncovalently to the protein (at a rate of  $K_i$ ), placing the reactive electrophilic group ( $\Delta^{12(13)}$  exocyclic double bond of **1**) close to the nucleophilic residue (Cys62 of NF- $\kappa$ B p50). A covalent bond then forms (at a rate of  $k_2$ ) to generate the adduct. Unlike highly electrophilic compounds that react nonspecifically with exposed nucleophilic residues, this class of covalent drug depends on both  $K_i$  and  $k_2$  and are thus termed targeted covalent inhibitors.  $K_i$  must be sufficient to allow for selective binding and residence time for the formation of the covalent bond, and  $k_2$  must allow for the presence of a reaction within the lifetime of the noncovalent complex, without forming nonspecific covalent bonds with any thiol groups.

The importance of the first step ( $K_i$ ) is evident from our observation that **1** targets NF- $\kappa$ B p65 only weakly (see Supporting Information). The Cys38 of p65 is strongly targeted by the sesquiterpene lactones (see Supporting Information), which have a distinct structure from that of **1**,<sup>27</sup> and thus the drug binding sites of p65 and p50 are expected to differ. In other protein families, such as serine or cysteine proteases, inhibitors that target the active site will likely have multiple off-target effects because of the similar active sites and conserved residues among the proteases.<sup>28</sup>

**Reactivity and Mechanism of Interaction of Analogues of Andrographolide (1) with NF- $\kappa$ B p50.** Mass spectrometry was used to determine the relative reactivity of **1** and several of its analogues on p50, including **4–10** (Table 1).

**Table 1. Reactivity, Secreted Alkaline Phosphatase (SEAP) Activity, and Cytotoxicity of the Various Analogues of Andrographolide (1) with NF- $\kappa$ B p50<sup>a</sup>**

compound	reactivity with NF- $\kappa$ B p50	SEAP assay activity	cytotoxicity	shift in molecular weight (MW) (Da)	difference from theoretical MW (Da)
<b>1</b>	+++	++	+	332	-18
<b>4</b>	-	-	-	N.A.	N.A.
<b>5</b>	-	-	-	N.A.	N.A.
<b>6</b>	+++	+++	+++	417	0
<b>7</b>	-	-	-	N.A.	N.A.
<b>8</b>	+	-	-	348	+16
<b>9</b>	-	-	-	N.A.	N.A.
<b>10</b>	-	-	-	N.A.	N.A.

<sup>a</sup>The shifts in molecular weight of NF- $\kappa$ B after reaction with the various analogues of **1** are listed, and the differences from theoretical molecular weight are calculated. "N.A." stands for "not applicable", as reactions of these analogues with NF- $\kappa$ B p50 were not observed.

On the basis of the mass spectra, in addition to **1**, compounds **6** and **8** both showed observable reactions with p50 at the concentrations tested. Compound **8** was found to be much less reactive than **1**, and saturation could not be achieved even up to a molar ratio of 50:1 (Figure 3A). Compound **6** reacted with p50 NTD with similar or even better reactivity than **1**, with saturation achieved at 4:1 (Figure 3B). The other analogues did not react with p50 NTD up to a molar ratio of 10:1 (Figure 3C).

A novel oxidative modification was previously determined for redox-active cysteine residues using a shift in the molecular weight as an indicator.<sup>29</sup> To provide further insight into the mechanism of reaction of each analogue of **1** with p50, the shift

in the molecular weight of the adduct was measured and compared with the theoretical molecular weight (Table 1). The NF- $\kappa$ B p50-**1** adduct showed a shift of -18 Da, which is consistent with the Michael addition reaction proposed by Zhang and colleagues described above.<sup>17</sup> Interestingly, a +16 Da molecular weight shift for **8** with p50-NTD was observed (Figure 3A), suggesting a mechanism different from that of **1**. To deduce this reactive mechanism, the location of the reactive site was determined by titrating cysteamine into analogues of **1** in DMSO- $D_6$  and monitoring the chemical shift perturbation using <sup>1</sup>H NMR.<sup>30</sup> The peaks that shifted or disappeared in the spectra represent sites that are modified by the addition of the nucleophilic cysteamine. For **8**, the C-15 proton peak disappeared after titration with cysteamine (Figure 3D); this may result from a putative mechanism<sup>31</sup> involving opening of the furan ring and nucleophilic attack at C-14 of **8** through a Michael addition by the -SH group of Cys62 of p50 (Figure 3D). On this basis, the addition of an oxygen atom (+16 Da) would cause an appropriate change in the molecular weight and also the disappearance of both the C-14 and C-15 proton peaks in the NMR spectrum. However, the C-14 proton peak did not disappear, suggesting that the reaction of **8** with cysteamine and NF- $\kappa$ B p50 may not follow the mechanism proposed. The reaction rate  $k_2$  for this particular reaction may be slower than that for **1** and could explain the relatively weaker reactivity of **8**. Any modifications to **8** to change the  $k_2$  may also affect the  $K_i$ , and these factors need to be considered when optimizing a new drug.

For **6**, the adduct that formed with p50 NTD has an identical molecular weight to the theoretical value, suggesting that **6** follows yet another mechanism, for which we hypothesize a Michael addition at the double bond between C-12 and C-13 but without the subsequent dehydration (Figure 3E). The necessity of the first noncovalent step ( $K_i$ ) may explain why **6** reacts strongly with p50 but the other analogue **7** cannot. The two acetate groups in C-3 and C-19 of **6** are replaced with two hydroxy groups in **7**, and these groups are too far away from the double bond between C-12 and C-13 to affect its electrophilicity. The two acetate groups of **6** likely interact with certain residues on p50, leading to a much higher  $K_i$  as compared to that of **7**.

The other analogues did not show any significant reaction with Cys62 of p50 (Table 1). For 14-deoxyandrographolide (**9**) and neo-andrographolide (**10**), both compounds lack the alkene double bond between C-12 and C-13 that may be needed to stabilize the transition state carbanion, which may explain why no adduct formation was observed with p50 for these analogues. A previous cytotoxicity study on a series of analogues of **1** (modified at the C-14 hydroxy group) revealed that attachment of the  $\alpha$ -alkylidene part (double bond between C-12 and C-13) to the  $\gamma$ -butyrolactone ring was crucial for the drug's cytotoxicity.<sup>32</sup> Others have shown that **10** and andrograpanin, both of which also lack the double bond, fail to inhibit LPS-induced cytokine release in macrophages<sup>33</sup> and that 4-hydroandrographolide, also missing the double bond, is an inactive analogue of **1**.<sup>14,34</sup>

**Importance of the Redox State of Cys62 of p50 for Binding of Andrographolide (1).** Evidence suggested that the RxxRxxR motif (Arg54 to Arg59) that precedes Cys62 of NF- $\kappa$ B is essential for DNA binding and redox regulation.<sup>15</sup> In NF- $\kappa$ B p50, only Cys62 lies adjacent to the highly conserved RxxRxxR sequence, and these Arg residues likely reduce its p $K_a$  and generate a "redox-active Cys".<sup>29</sup> To show that the RxxRxxR

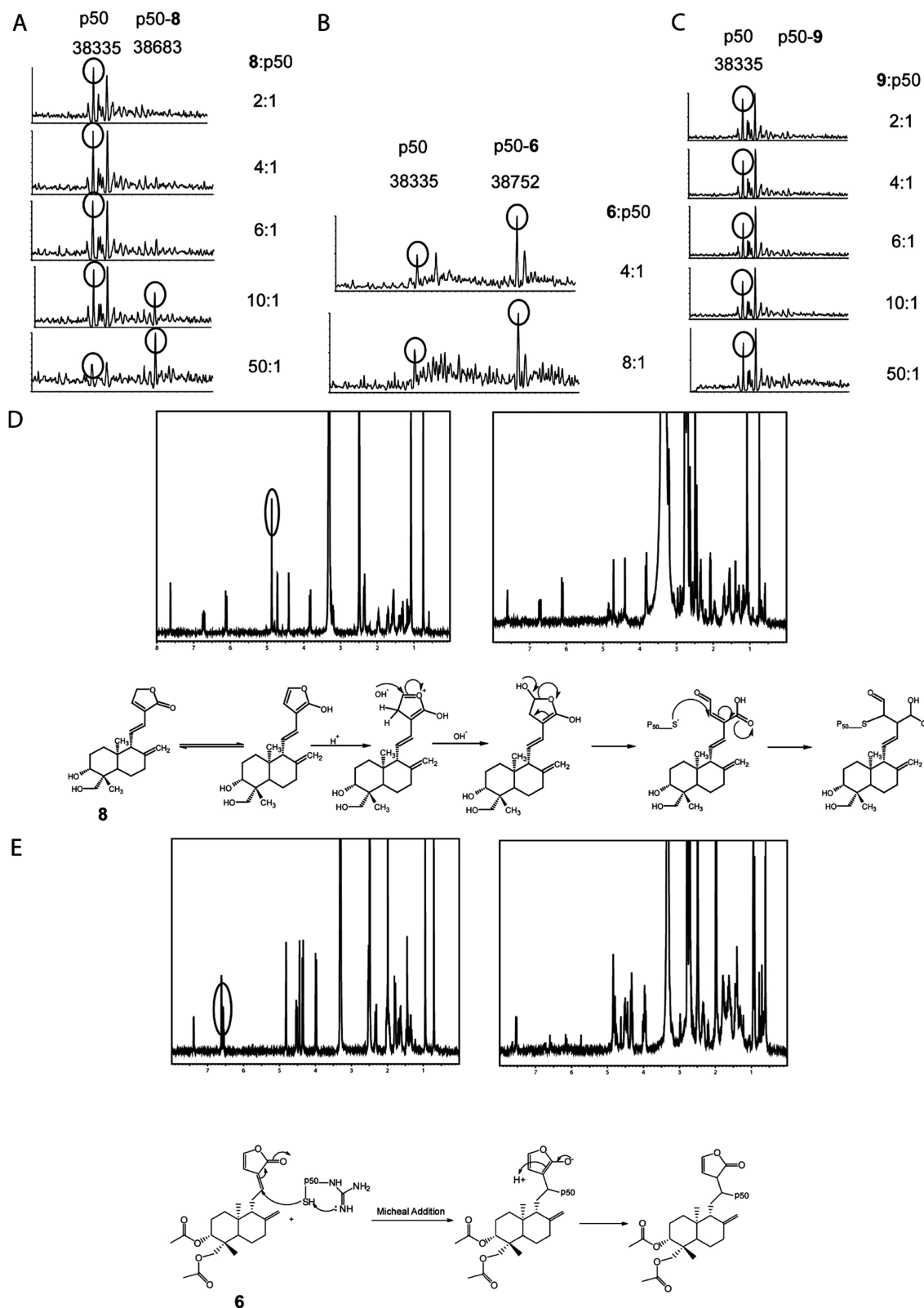


**Figure 3.** Reactivity and mechanism of reaction of andrographolide (1) analogues to NF- $\kappa$ B p50. Series of mass spectra showing the reaction of (A) 8, (B) 6, and (C) 9 with p50. The peaks of free p50 and the p50 adduct are marked by black circles with their respective molecular weights shown above. The molar ratios of analogue:p50 are shown at the right-hand side of each mass spectrum. (D) NMR spectra of 8 before (left) and after (right) reaction with cysteamine. The peak for the C-15 proton of 8 (circled in black) at 4.88 ppm is absent. Proposed mechanism of reaction between 8 and p50 with a molecular weight gain of 16 Da in the final complex. (E) NMR spectra of 6 before (left panel) and after (right panel) reaction with cysteamine. The peak for the C-12 proton of 6 (circled in black) at 6.57 ppm is absent. Proposed mechanism of reaction between 6 and p50 without a gain or loss in the molecular weight of the final complex.

motif is directly involved in the reaction between **1** and Cys62 of p50, we performed site-directed mutagenesis on residues Arg57 and Arg59 of the RxxRxR. Mutation of either residue to Ala significantly affected the reaction between **1** and p50, as observed using mass spectrometry (Figure 4A and B).

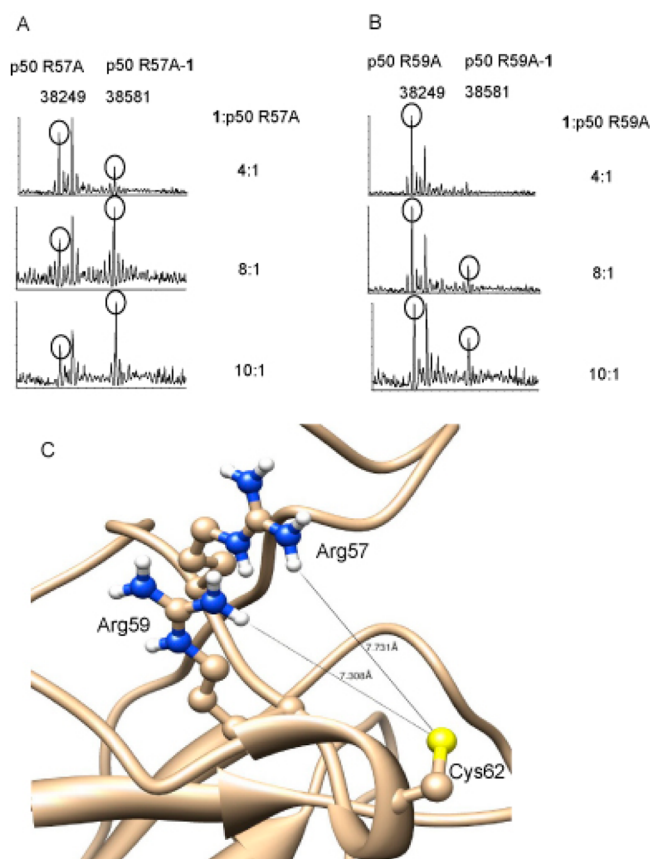


**Figure 4.** Importance of Arg residues in the RxxRxR motif on the reactivity of andrographolide (**1**) to p50. A series of mass spectra showing the reaction of **1** with (A) R57A and (B) R59A mutants of p50. The peaks of free p50 and the p50-**1** adduct are marked with black circles with their respective molecular weights shown above. The molar ratios of **1**:p50 are shown at the right-hand side of each mass spectrum. (C) Ribbon diagram showing the positions of residues Arg57 and Arg59 relative to Cys62. The approximate distances from the side chains of these two Arg residues (7.731 and 7.308 Å, respectively) to Cys62 are indicated by dotted lines. The figure is generated using the program Chimera.<sup>25</sup>

However, although the distances from the side-chains of Arg57 or Arg59 to Cys62 are similar in the crystal structure (Figure 4C), the reaction was especially affected by the R59A mutation, suggesting that the actual distances of Arg59 to Cys62 may be shorter than the crystal structure indicates or that Arg59 is performing a different role from Arg57 in the binding.

As the redox state of Cys62 is essential for the reaction of **1** with p50, we next sought to determine whether the reactivity is affected by the presence of different concentrations of two reducing agents:  $\beta$ -mercaptoethanol and DTT. We found that there is no reaction if either  $\beta$ -mercaptoethanol or DTT is excluded from the reaction; a small amount of  $\beta$ -mercaptoethanol (10–100  $\mu$ M) is needed to reduce the Cys62 residue to achieve optimal results. However, too much  $\beta$ -mercaptoethanol (10 mM) can inhibit the reaction, with 100 mM terminating

the reaction completely (Figure 5A). A similar effect was observed with DTT, only the reducing power was almost 10 times stronger than that of  $\beta$ -mercaptoethanol (Figure 5B). Our results are in agreement with the findings of others.<sup>14</sup>

Cys is exploited as a redox sensor by the body to regulate NF- $\kappa$ B DNA binding and the transcription of many genes, whereas most Cys-containing proteins localize in the cytoplasm in a reduced state. Cys62 is highly oxidized or modified to prevent DNA binding and thus needs to be reduced, for example, by thioredoxin, before it can bind DNA.<sup>35</sup> In addition to oxidation, S-glutathionylation of p50 at Cys62 is also involved in the redox regulatory mechanisms of NF- $\kappa$ B.<sup>36</sup> Substitution of the “redox-active” Cys residue with Ser enables v-Rel to escape redox control, thus promoting overall DNA binding.<sup>15</sup> Pande and colleagues show that direct covalent modification of the redox-regulated Cys62 inhibits NF- $\kappa$ B and DNA binding.<sup>37</sup> Here, too, we found that, in addition to DNA binding, Cys62 needs to be reduced to covalently react with **1** to inhibit DNA binding, similar to other types of Cys modifications used by NF- $\kappa$ B.

Previous reports suggest that the Michael addition may be reversible through hydrolysis of the adduct.<sup>38,39</sup> To determine if the adduct formed between **1** and p50 could be dissociated, different concentrations of DTT were added to the formed NF- $\kappa$ B p50-**1** adduct, and the amount of free p50 was measured using mass spectrometry. The results showed that the covalent adduct formed between **1** and p50 could indeed be dissociated by DTT (Figure 5C), with complete dissociation within 2 h using 5 mM DTT (Figure 5C). Under *in vitro* cell assay, **1** may react with other biomolecules in the cell and the reversibility of these reactions could affect the bioavailability and reactivity of the drug. GSH is the most abundant nonprotein thiol in eukaryotic cells,<sup>39</sup> which protects cells by detoxifying electrophilic compounds and acts as an antioxidant. GSH is depleted during attacks by electrophilic compounds, commonly by alkylation mechanisms.<sup>40</sup> Compound **1** likely reacts with GSH, and so the reversible dissociation of the GSH-**1** complex is essential for the bioavailability of **1** for its inhibition of NF- $\kappa$ B. When designing an electrophilic drug, the ease of dissociation from GSH or the protein target should therefore be considered.

**Compound 6 and Andrographolide (1) React Strongly with p50 in *in Vitro* Cell Assay.** The inhibitory activity of **1** and its analogues was investigated using a secreted alkaline phosphatase (SEAP) reporter assay.<sup>41</sup> Cells were transfected with the pNF- $\kappa$ B/SEAP plasmid and induced with TNF- $\alpha$ . Both **1** and **6** reacted strongly with p50 in a SEAP activity assay with IC<sub>50</sub> values of 49.6  $\pm$  61.7 and 11.1  $\pm$  7.3  $\mu$ M, respectively (Figure 6A and C). Although **8** reacted weakly with p50 in the mass spectrometry results, SEAP activity was unaffected, even with concentrations up to 100  $\mu$ M (Figure 6B). Compounds **4**, **5**, and **7** did not inhibit SEAP activity, and this was expected, given their lack of reactivity with p50 in a cell-free assay (Figure 6D, E, and F). The results suggest that there is a general correlation between the results obtained from the *in vitro* SEAP reporter assay and the cell-free mass spectrometry assay in detecting the interaction of **1** and its analogues with p50 (Table 1).

**Compound 6 Exhibits Higher Cytotoxicity.** Finally, the cytotoxicity of the interaction was assessed, as this will affect the suitability of a small-molecule inhibitor as an antiasthma agent. Flow cytometry, with propidium iodide staining and annexin V binding to phosphatidyl serine, was used to ascertain the cytotoxicity of **1** and its analogues. No correlation was

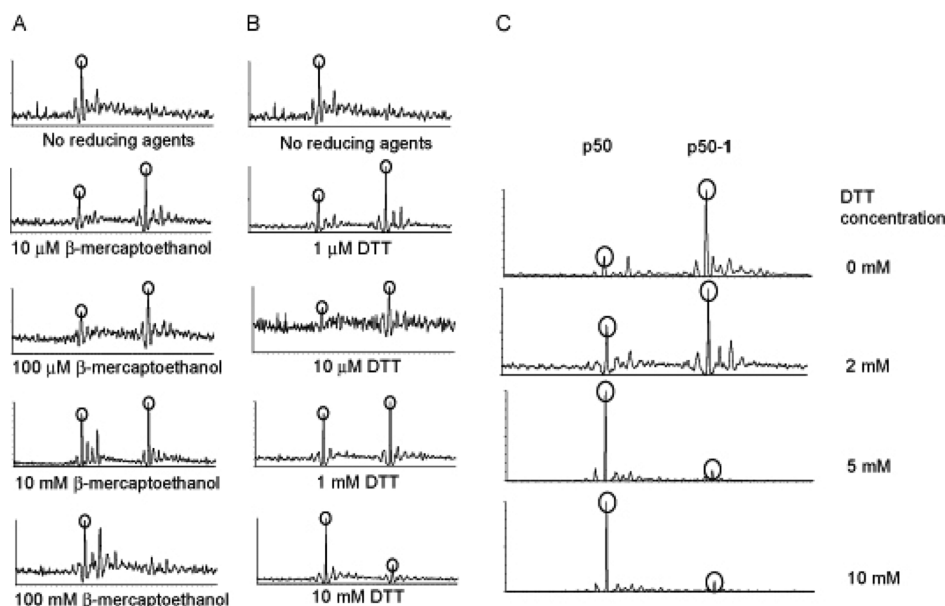


**Figure 5.** Importance of redox conditions on the interaction between andrographolide (**1**) and p50. A series of mass spectra showing the reaction of **1** with p50 in the presence of various concentrations of (A)  $\beta$ -mercaptoethanol and (B) DTT at a molar ratio of 1:p50 = 4:1. The peaks of free p50 and the p50–**1** adduct are marked with black circles. (C) Dissociation of preformed p50–**1** adduct in the presence of various concentrations of DTT. The peaks of free p50 and the p50–**1** adduct are marked with black circles.

found between cytotoxicity and reactivity for **1** and **6**, but the cytotoxicity of **6** was significantly higher than that of **1**, as shown by the higher amount of late apoptosis/necrosis (Figure 7A and C). This higher cytotoxicity for **6** likely contributes to the inhibition of the SEAP reporter assay, although we did not confirm a direct interaction between **6** and NF- $\kappa$ B p50. The higher cytotoxicity of **6** is possibly caused by the presence of other cellular targets for **6**. Compounds **8**, **4**, **7**, and **5**, which had low or no reactivity, also, not surprisingly, had a comparatively lower cytotoxicity (Figure 7B, D, E, and F). None of the analogues had high cytotoxicity with low reactivity. Thus, our findings suggest that cytotoxicity may be related to electrophilicity of this class of compounds. However, the exact mechanism and cellular targets leading to this cytotoxicity remain to be determined.

Compound **6** has a much higher cytotoxicity than **1** or **8**, and it is therefore not suitable for the treatment of asthma. Although **6** should have a similar electrophilicity to **1**, we found that the  $K_i$  of **6** for NF- $\kappa$ B p50 and the reversibility of the NF- $\kappa$ B p50–**6** complex are likely to be different from those of **1**. The cytotoxicity of covalent modifiers can be reduced by reducing the intrinsic electrophile reactivity ( $k_2$ ) to avoid nonspecific interactions with off targets. However, following appropriate positioning ( $K_i$ ) on the target protein, the modifier should react selectively with the nucleophile.<sup>42</sup> Cytotoxicity is found to be quantitatively correlated with the electrophilicity index, and the model can be applied to a series of electrophilic compounds in terms of their interactions with biological nucleophilic targets.<sup>43</sup> In addition to NF- $\kappa$ B, **1** has multiple cellular targets against inflammation;<sup>44</sup> for instance, it inhibits TNF- $\alpha$ -induced inflammation by down-regulating the PI3K/Akt signaling pathway.<sup>45</sup> The profiles of protein targets and their binding sites for **1** and other electrophilic drugs will need to be characterized to understand the factors that affect specificity, reactivity, and cytotoxicity of this family of compounds.

## EXPERIMENTAL SECTION

**Expression and Purification of NF- $\kappa$ B p50.** Human NF- $\kappa$ B p50 DNA was a generous gift from Prof. Gourisankar Ghosh (University of California at San Diego). The RHR DNA (residues 39–364) of NF- $\kappa$ B p50 NTD was subcloned into pET-M (a modified pET-32a vector with thioredoxin and S-tag removed) and subsequently transformed into *E. coli* BL21(DE3) cells. The protein was subsequently expressed using IPTG according to standard practices. The cells were resuspended in Ni-binding buffer containing 20 mM Tris-HCl, pH 8.0, 0.5 M NaCl, and 5 mM imidazole, lysed by sonication on ice, and then centrifuged at 18000g for 30 min. The supernatant was loaded onto Ni-NTA columns (Qiagen, Valencia, CA, USA), and the columns were washed 10 times with a total volume of 500 mL of Ni washing buffer containing 20 mM Tris-HCl, pH 8.0, 0.5 M NaCl, and 30 mM imidazole to remove unbound proteins. Recombinant p50 NTD with a 6-His tag was eluted with 20 mM Tris-HCl, pH 8.0, 0.5 M NaCl, and 500 mM imidazole. The eluted p50 NTD protein was dialyzed against phosphate-buffered saline (PBS) to remove the imidazole. p50 NTD was further purified using a HiLoad 16/60 Superdex 200 gel filtration column (GE Healthcare, Piscataway, NJ, USA). p50 NTD in PBS was stored at  $-80^\circ\text{C}$ .

**Synthesis of Analogues of Andrographolide (**1**).** Andrographolide (**1**) at 98% purity was purchased from Sigma-Aldrich (St. Louis, MO, USA). 14-Deoxy-11,12-didehydroandrographolide (**8**), 14-deoxyandrographolide (**9**), and neo-andrographolide (**10**) at >98% purity were purchased from TCM Institute of Chinese Materia Medica (Nanjing, China). The Supporting Information provides a detailed description of the synthesis of analogues of **1** (**4**, **5**, **6**, and **7**). Solutions (100 mM) of each were prepared by dissolving the powder in DMSO.

**Computer Docking.** The crystal structure of NF- $\kappa$ B p50 (PDB ID: 1NFK) was used for docking **1** with iGEMDOCK 2.1.<sup>24</sup> The 3D structure of **1** was generated using the PRODRG server (<http://davapc1.bioch.dundee.ac.uk/prodrg/>).<sup>46</sup> “Accurate docking” was used, with a population size of 800 and generations of 80. The number of solutions was increased to 100 for more reliable clustering. This was a blind docking without specifying the locations of the binding site or the interacting residues.

**Site-Directed Mutagenesis.** Mutations at the predicted binding site of **1** and the RxxRxR motif were performed using PCR-based site-

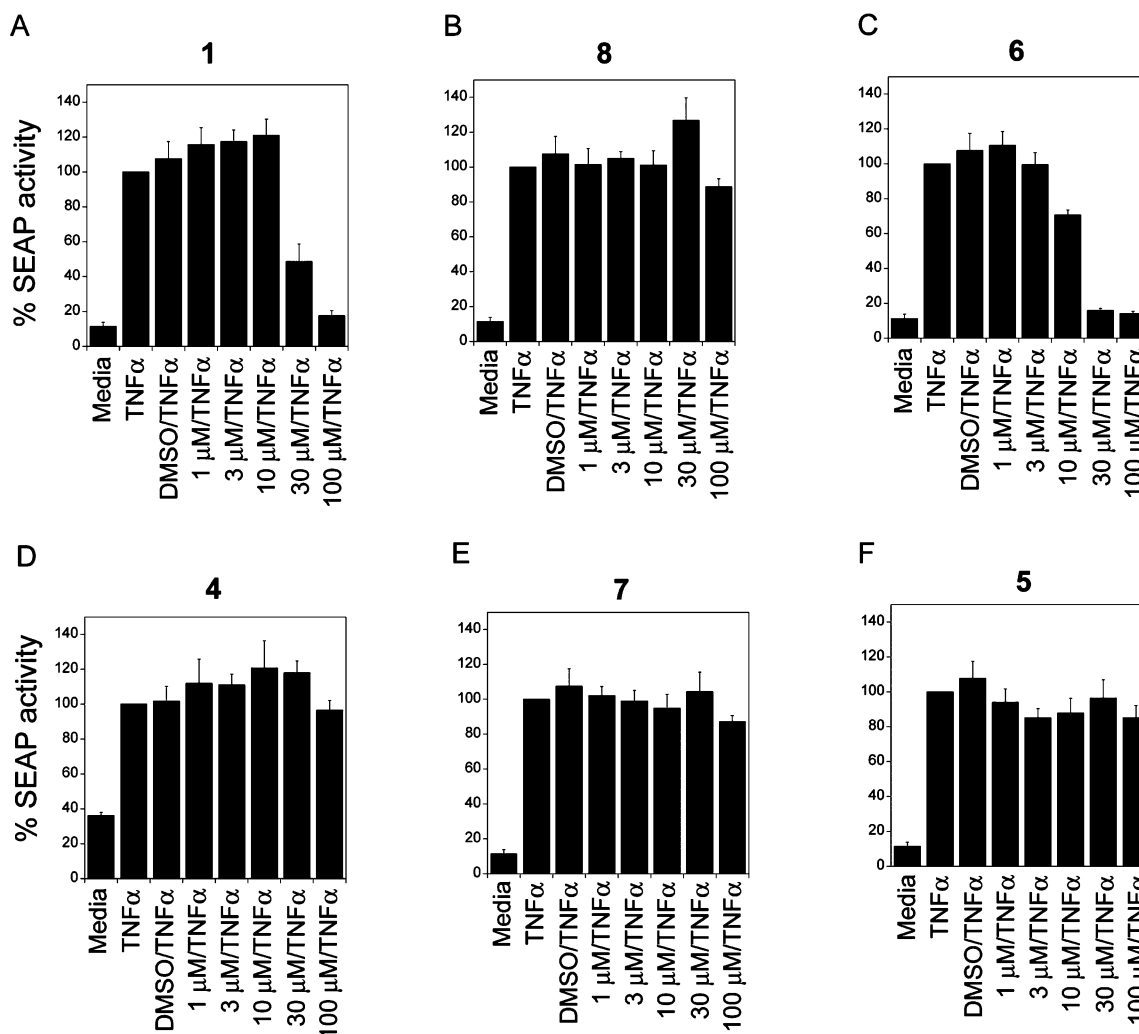


**Figure 6.** SEAP reporter assay showing the inhibitory activities of andrographolide (**1**) and its analogues on p50. SEAP reporter assays were performed to determine the *in vitro* inhibitory activities of (A) **1**, (B) **8**, (C) **6**, (D) **4**, (E) **7**, and (F) **5** on NF- $\kappa$ B p50 using HEK293 cells transfected with the pNF- $\kappa$ B/SEAP plasmid and induced with TNF- $\alpha$ . The SEAP activity from TNF- $\alpha$ -induced cells without any additive was counted as 100% SEAP activity. The concentrations of **1** and its analogues are shown on the x-axis. “Media” represents SEAP activity from cells before TNF- $\alpha$  induction. “DMSO” represents SEAP activity from cells in the presence of 0.05% DMSO. Results are presented as the mean of quadruplicates. The IC<sub>50</sub> values of compounds **1** and **6** on NF- $\kappa$ B p50 are determined to be  $49.6 \pm 61.7$  and  $11.1 \pm 7.3$   $\mu$ M, respectively.

directed mutagenesis and complementary primers with mismatched bases. PCR was performed using the high-fidelity KOD Hot Start Pfu DNA polymerase (Novagen, Madison, WI, USA). Methylated wild-type plasmids were digested with 1  $\mu$ L of 1 U Fast Digest Dpn I at 37  $^{\circ}$ C for 1 h. Mutated plasmids were transformed into *E. coli* DH5 $\alpha$  competent cells on LB agar with ampicillin. Mutations were verified by DNA sequencing. Double mutants were generated using the mutated plasmids as starting DNA templates.

**Mass Spectrometry.** For each reaction, **1** or its analogues were incubated with 1 mL of p50 NTD (20  $\mu$ M) in PBS containing 1 mM EDTA, 10  $\mu$ M  $\beta$ -mercaptoethanol, and 5% glycerol (v/v) at 37  $^{\circ}$ C for 2 h. Glacial acetic acid (100  $\mu$ L) was added, and the samples were filtered and injected into a reversed-phase column (Atlantis Columns, dC18, 4.6  $\times$  250 mm, 5  $\mu$ m, Waters Corporation, Manchester, UK) pre-equilibrated with H<sub>2</sub>O containing 0.1% trifluoroacetic acid (TFA). p50 NTD was eluted using a gradient of 0–100% absolute acetonitrile containing 0.1% TFA and then collected and analyzed by a Synapt HDMS mass spectrometer (Waters Corporation). The samples were directly injected into the ESI source. The ESI QTOF-mass spectrometer was operated in positive ion mode using the following optimized conditions: flow rate, 40  $\mu$ L/min; source temperature, 80  $^{\circ}$ C; source spray voltage, 3.5 kV; desolvation gas temperature, 150  $^{\circ}$ C; cone gas flow, 50 L/h; desolvation gas flow, 100 L/h; capillary voltage,

3.5 kV; sampling cone voltage, 35 V; and extraction cone voltage, 6.0 V. Data were acquired between *m/z* 500 and 3000 Da and processed using MassLynx 4.1 software (Waters Corporation). For dissociation of the NF- $\kappa$ B p50–1 complex with DTT, the NF- $\kappa$ B p50–1 complex was formed by incubating an excess amount of **1** (20:1) with p50 NTD for 2 h. The unbound **1** was removed by dialysis three times with PBS. The NF- $\kappa$ B p50–1 complex was further purified using a HiLoad 16/60 Superdex 200 gel filtration column (GE Healthcare). Complete formation of the complex was confirmed by mass spectrometry. The complex was tested for dissociation by incubating with different concentrations of DTT for 2 h at 37  $^{\circ}$ C in PBS containing 1 mM EDTA, 10  $\mu$ M  $\beta$ -mercaptoethanol, and 5% glycerol (v/v). Samples were purified using a reversed-phase chromatography column (Waters Corporation, Milford, MA, USA), as described above for mass spectrometry analysis.

**NMR Titration with Cysteamine.** Compounds **1**, **6**, and **8** were prepared as 100 mM stock solutions in DMSO-*D*<sub>6</sub> (Sigma-Aldrich). Individual reactions were prepared with 2 mM of each drug treated with an excess amount of cysteamine (Sigma-Aldrich) at a final concentration of 10 mM in 500  $\mu$ L of DMSO-*D*<sub>6</sub>. The reaction was monitored using <sup>1</sup>H NMR spectra after 30 min incubation at 37  $^{\circ}$ C. As a control, the <sup>1</sup>H NMR spectrum of each drug before the addition of cysteamine was also recorded.

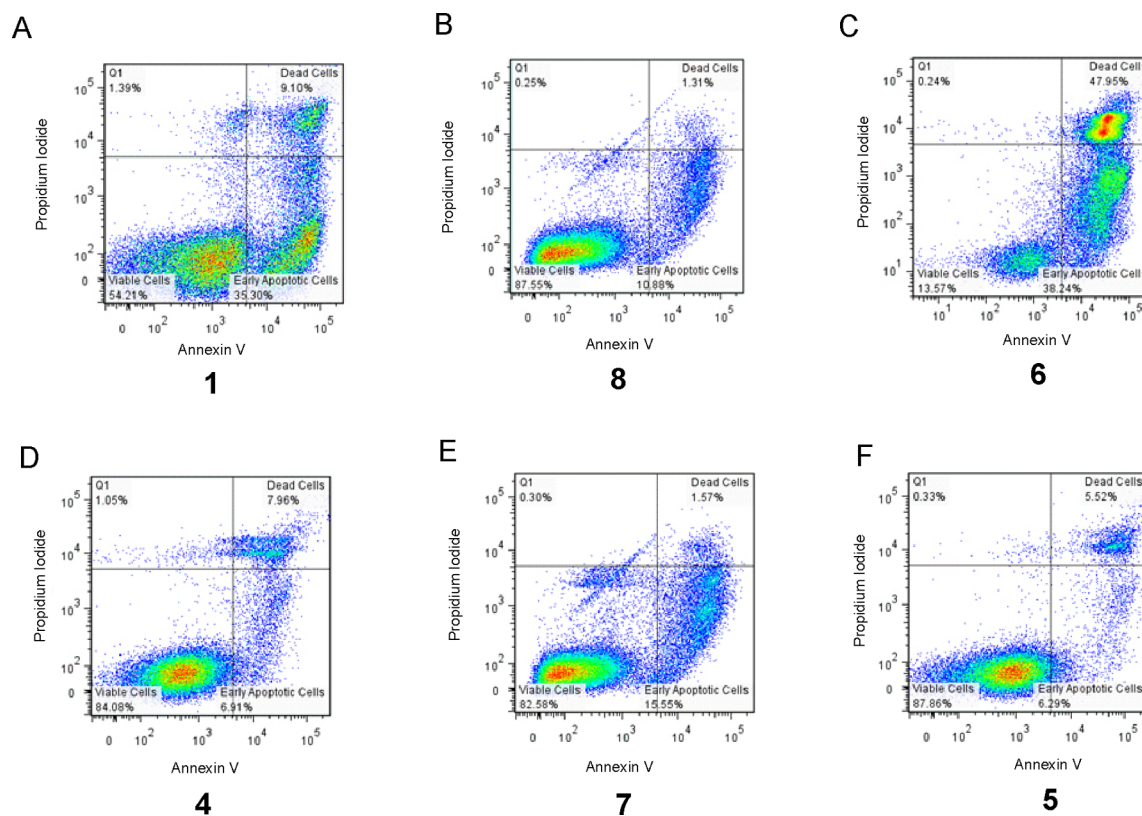


**Figure 7.** Cytotoxicity of andrographolide (**1**) and its analogues as determined by flow cytometry. Flow cytometry was performed to determine the cytotoxicity of 25  $\mu$ M of (A) **1**, (B) **8**, (C) **6**, (D) **4**, (E) **7**, and (F) **5** on Jurkat cells after 24 h incubation. The cells were stained with annexin-V-FLUOS and propidium iodide. The x-axis represents increasing annexin-V-FLUOS fluorescence, and the y-axis represents increasing propidium iodide fluorescence. Viable cells are both negative for propidium iodide and annexin-V-FLUOS staining.

**SEAP Reporter Assay for NF- $\kappa$ B Inhibition.** NF- $\kappa$ B/SEAP stably transfected HEK293 cells (Imgenex, San Diego, CA, USA) were grown at 37  $^{\circ}$ C and 5% CO<sub>2</sub> in DMEM supplemented with 10% FBS, 1% streptomycin/penicillin, and 500  $\mu$ g/mL G418 (Life Technologies, Carlsbad, CA, USA). Cells were seeded into the wells of a 24-well plate ( $\sim 2 \times 10^5$  cells per well) and grown to  $\sim 70\%$  confluence. After pretreatment with increasing concentrations of **1**, its analogues, or vehicle control (0.05% DMSO) for 4 h, TNF- $\alpha$  (10 ng/mL, Invitrogen, Carlsbad, CA, USA) was added to the cells for another 24 h to stimulate NF- $\kappa$ B activity and SEAP protein expression. SEAP levels were detected using the SEAPorter assay kit (Novus Biologicals, Littleton, CO, USA) according to the manufacturer's protocol.

**Cytotoxicity Assay.** Jurkat T lymphocytes (ATCC, Manassas, VA, USA) were cultured at 37  $^{\circ}$ C and 5% CO<sub>2</sub> in RPMI1640 medium supplemented with 10% FBS and 1% streptomycin/penicillin. Cells were incubated with 25  $\mu$ M **1** or its analogues for 24 h before cytotoxicity assays were performed. Cells were stained with annexin-V-FLUOS and propidium iodide according to the manufacturer's protocol (Roche Diagnostics, Mannheim, Germany). Apoptotic cells were detected using the Becton-Dickinson LSR Fortessa flow cytometer (BD Biosciences, San Jose, CA, USA) and analyzed using FlowJo software (Tree Star Inc., Ashland, OR, USA).

## ■ ASSOCIATED CONTENT

### 📄 Supporting Information

Detailed schemes for chemical synthesis of analogues of andrographolide, far-UV CD spectra of wild-type, S66A, and I142A mutants of NF- $\kappa$ B p50, and mass spectra showing reaction of NF- $\kappa$ B p65 with andrographolide and the two sesquiterpene lactones, parthenolide and hehelenin, are presented. This material is available free of charge via the Internet at <http://pubs.acs.org>.

## ■ AUTHOR INFORMATION

### Corresponding Author

\*Tel: +65 6516 2967. Fax: +65 6779 2486. E-mail: [dbsmkh@nus.edu.sg](mailto:dbsmkh@nus.edu.sg).

### Present Address

<sup>†</sup>Faculty of Biology, Hanoi University of Sciences, Vietnam National University, 334 Nguyen Trai, Thanh Xuan, Ha Noi, Vietnam.

### Notes

The authors declare no competing financial interest.

## ■ ACKNOWLEDGMENTS

This study was supported by grants from the Biomedical Research Council (BMRC/09/1/21/19/595) and the Cross-Faculty Research Grant (R-184-000-193-646) to W.S.F.W. The DNA template for human NF $\kappa$ B p50 was a generous gift from Prof. G. Ghosh at UCSD. We thank Dr. Kim C.-Y., Ms. Fang M.Y., and Mr. A. Mahmoud Mohammed Sayed for deducing the mechanisms of reaction between NF- $\kappa$ B p50 and the analogues of **1**.

## ■ REFERENCES

- (1) Huxford, T.; Ghosh, G. *Cold Spring Harb. Perspect. Biol.* **2009**, *1*, a000075.
- (2) Berkowitz, B.; Huang, D.-B.; Chen-Park, F. E.; Sigler, P. B.; Ghosh, G. *J. Biol. Chem.* **2002**, *277*, 24694–24700.
- (3) Chen, F. E.; Huang, D.-B.; Chen, Y.-Q.; Ghosh, G. *Nature* **1998**, *391*, 410–413.
- (4) Chen, Y.-Q.; Sengchanthalangsy, L. L.; Hackett, A.; Ghosh, G. *Structure* **2000**, *8*, 419–428.

- (5) Müller, C. W.; Rey, F. A.; Sodeoka, M.; Verdine, G. L.; Harrison, S. C. *Nature* **1995**, *373*, 311–317.
- (6) Ghosh, G.; Van Duynne, G.; Ghosh, S.; Sigler, P. B. *Nature* **1995**, *373*, 303–310.
- (7) Phelps, C. B.; Sengchanthalangsy, L. L.; Malek, S.; Ghosh, G. J. *Biol. Chem.* **2000**, *275*, 24392–24399.
- (8) Chen, F. E.; Ghosh, G. *Oncogene* **1999**, *18*, 6845–6852.
- (9) Ghosh, S.; May, M. J.; Kopp, E. B. *Annu. Rev. Immunol.* **1998**, *16*, 225–260.
- (10) Pande, V.; Ramos, M. J. *Curr. Med. Chem.* **2005**, *12*, 357–374.
- (11) Lim, J. C. W.; Chan, T. K.; Ng, D. S. W.; Sagineedu, S. R.; Stanslas, J.; Wong, W. S. F. *Clin. Exp. Pharmacol. Physiol.* **2012**, *39*, 300–310.
- (12) Barrett, A. J.; Kembhavi, A. A.; Brown, M. A.; Kirschke, H.; Knight, C. G.; Tamai, M.; Hanada, K. *Biochem. J.* **1982**, *201*, 189–198.
- (13) Gersch, M.; Kreuzer, J.; Sieber, S. A. *Nat. Prod. Rep.* **2012**, *29*, 659–682.
- (14) Xia, Y.-F.; Ye, B.-Q.; Li, Y.-D.; Wang, J.-G.; He, X.-J.; Lin, X.; Yao, X.; Ma, D.; Slungaard, A.; Hebbel, R. P.; Key, N. S.; Geng, J.-G. *J. Immunol.* **2004**, *173*, 4207–4217.
- (15) Kumar, S.; Rabson, A. B.; Gélinas, C. *Mol. Cell. Biol.* **1992**, *12*, 3094–3106.
- (16) Yao, H.; Li, S.; Yu, P.; Tang, X.; Jiang, J.; Wang, Y. *Molecules* **2012**, *17*, 728–739.
- (17) Zhang, Z.; Chan, G. K.-L.; Li, J.; Fong, W.-F.; Cheung, H.-Y. *Chem. Pharm. Bull.* **2008**, *56*, 1229–1233.
- (18) Bao, Z.; Guan, S.; Cheng, C.; Wu, S.; Wong, S. H.; Kemeny, D. M.; Leung, B. P.; Wong, W. S. F. *Am. J. Resp. Crit. Care* **2008**, *179*, 657–665.
- (19) Guan, S.-P.; Kong, L.-R.; Cheng, C.; Lim, J. C. W.; Wong, W. S. F. *J. Nat. Prod.* **2011**, *74*, 1484–1490.
- (20) Wang, Y.-J.; Wang, J.-T.; Fan, Q.-X.; Geng, J.-G. *Cell Res.* **2007**, *17*, 933–941.
- (21) Sirion, U.; Kasemsook, S.; Suksen, K.; Piyachaturawat, P.; Suksamrarn, A.; Saeeng, R. *Bioorg. Med. Chem. Lett.* **2012**, *22*, 49–52.
- (22) Dey, S. K.; Bose, D.; Hazra, A.; Naskar, S.; Nandy, A.; Munda, R. N.; Das, S.; Chatterjee, N.; Mondal, N. B.; Banerjee, S.; Saha, K. D. *PLoS One* **2013**, *8*, e58055.
- (23) Wong, C. C.; Sagineedu, S. R.; Sumon, S. H.; Sidik, S. M.; Phillips, R.; Lajis, N. H.; Stanslas, J. *Env. Toxicol. Pharmacol.* **2014**, *38*, 489–501.
- (24) Yang, J.-M.; Chen, C.-C. *Proteins* **2004**, *55*, 288–304.
- (25) Pettersen, E. F.; Goddard, T. D.; Huang, C. C.; Couch, G. S.; Greenblatt, D. M.; Meng, E. C.; Ferrin, T. E. *J. Comput. Chem.* **2004**, *25*, 1605–1612.
- (26) Singh, J.; Petter, R. C.; Baillie, T. A.; Whitty, A. *Nat. Rev. Drug Discovery* **2011**, *10*, 307–317.
- (27) García-Piñeres, A. J.; Castro, V.; Mora, G.; Schmidt, T. J.; Strunck, E.; Pahl, H. L.; Merfort, I. *J. Biol. Chem.* **2001**, *276*, 39713–39720.
- (28) Turk, B. *Nat. Rev. Drug Discovery* **2006**, *5*, 785–799.
- (29) Jeong, J.; Jung, Y.; Na, S.; Jeong, J.; Lee, E.; Kim, M.-S.; Choi, S.; Shin, D.-H.; Paek, E.; Lee, H.-Y.; Lee, K.-J. *Mol. Cell. Proteomics* **2011**, *10*, 1–13.
- (30) Avonto, C.; Tagliatalata-Scafati, O.; Pollastro, F.; Minassi, A.; Di Marzo, V.; De Petrocellis, L.; Appendino, G. *Angew. Chem., Int. Ed.* **2011**, *50*, 467–471.
- (31) Mel'chin, V. V.; Butin, A. V. *Tetrahedron Lett.* **2006**, *47*, 4117–4120.
- (32) Das, B.; Chowdhury, C.; Kumar, D.; Sen, R.; Roy, R.; Das, P.; Chatterjee, M. *Bioorg. Med. Chem. Lett.* **2010**, *20*, 6947–6950.
- (33) Chandrasekaran, C. V.; Thiyagarajan, P.; Deepak, H. B.; Agarwal, A. *Int. Immunopharmacol.* **2011**, *11*, 79–84.
- (34) Wang, L.-J.; Zhou, X.; Wang, W.; Tang, F.; Qi, C.-L.; Yang, X.; Wu, S.; Lin, Y.-Q.; Wang, J.-T.; Geng, J.-G. *J. Dent. Res.* **2011**, *90*, 1246–1252.
- (35) Na, H.-K.; Surh, Y.-J. *Mol. Carcinog.* **2006**, *45*, 368–380.
- (36) Pineda-Molina, E.; Klatt, P.; Vázquez, J.; Marina, A.; de Lacoba, M. G.; Pérez-Sala, D.; Lamas, S. *Biochemistry* **2001**, *40*, 14134–14142.
- (37) Pande, V.; Sousa, S. F.; Ramos, M. J. *Curr. Med. Chem.* **2009**, *16*, 4261–4273.
- (38) Schmidt, T. J.; Lyß, G.; Pahl, H. L.; Merfort, I. *Bioorg. Med. Chem.* **1999**, *7*, 2849–2855.
- (39) Shi, B.; Greaney, M. F. *Chem. Commun.* **2005**, 886–888.
- (40) Schwöbel, J. A. H.; Wondrousch, D.; Koleva, Y. K.; Madden, J. C.; Cronin, M. T. D.; Schüürmann, G. *Chem. Res. Toxicol.* **2010**, *23*, 1576–1585.
- (41) Berger, J.; Hauber, J.; Hauber, R.; Geiger, R.; Cullen, B. R. *Gene* **1988**, *66*, 1–10.
- (42) Potashman, M. H.; Duggan, M. E. *J. Med. Chem.* **2009**, *52*, 1231–1246.
- (43) Campodónico, P. R.; Contreras, R. *Bioorg. Med. Chem.* **2008**, *16*, 3184–3190.
- (44) Wang, J.; Tan, X. F.; Nguyen, V. S.; Yang, P.; Zhou, J.; Gao, M.; Li, Z.; Lim, T. K.; He, Y.; Ong, C.-S.; Lay, Y.; Ghosh, D.; Mok, Y. K.; Shen, H.-M.; Lin, Q. *Mol. Cell. Proteomics* **2014**, *13*, 876–886.
- (45) Chen, H.-W.; Lin, A.-H.; Chu, H.-C.; Li, C.-C.; Tsai, C.-W.; Chao, C.-Y.; Wang, C.-J.; Lii, C.-K.; Liu, K.-L. *J. Nat. Prod.* **2011**, *74*, 2408–2413.
- (46) Schüttelkopf, A. W.; van Aalten, D. M. F. *Acta Crystallogr.* **2004**, *D60*, 1355–1363.